# Using the global positioning system to map disturbance patterns of forest harvesting machinery

**T.P. McDonald, E.A. Carter, and S.E. Taylor**

**Abstract**: A method was presented to transform sampled machine positional data obtained from a global positioning system (GPS) receiver into a two-dimensional raster map of number of passes as a function of location. The effect of three sources of error in the transformation process were investigated: path sampling rate (receiver sampling frequency); output raster resolution; and GPS receiver errors. Total accuracy of traffic maps across a site (the summed areas receiving one, two, three, etc. passes) was not greatly affected by the error sources. The estimate of number of passes at a specific point, however, was heavily dependent on the presence of errors in the input data. Adding random offsets to each GPS position, for example, resulted in less than a 35% chance that an individual pixel would be classified correctly following transformation when compared with a reference raster. Although the absolute accuracy of the GPS–transformation system was not defined, it was concluded that data derived from applying it could be used to make estimates of total site disturbance and to identify regions of higher or lower disturbance but was less effective when applied in defining number of passes at a given point in a stand.

**Résumé** : Les auteurs présentent une méthode de traitement de données GPS qui permet de convertir un échantillon de points de positionnement d'un équipement forestier, en une couverture matricielle relatant le nombre de passages selon la localisation. L'effet de trois sources d'erreurs dans le processus de transformation a été étudié : la fréquence d'échantillonnage du récepteur, la définition des pixels et l'erreur de réception du GPS. La précision de la cartographie des passages sur un site (sommation des surfaces ayant reçu un, deux, trois, … passages) n'est pas significativement affectée par ces sources d'erreurs. Toutefois, l'estimation du nombre de passages en un point spécifique est grandement influencée par la présence d'erreurs liées aux données sources. L'ajout de points aléatoires à chacune des positions GPS permet, par exemple, de réduire à moins de 35% la probabilité qu'un pixel soit classé correctement suite au traitement, comparativement à une référence matricielle. Bien que la précision absolue du système « GPS–transformation » n'ait pas été déterminée, les auteurs concluent que l'information extraite par cette méthode peut être utilisée pour estimer la perturbation infligée aux sites et identifier les sections de faible et de haute perturbations. La procédure s'est cependant avérée moins efficace pour définir le nombre de passages en un point donné, à l'intérieur d'un peuplement.

[Traduit par la Rédaction]

## Introduction

Preserving the overall health and quality of soils is a key component in maintaining long-term forest productivity. Consequently, impacts of forest management on soil characteristics, especially soil compaction from harvesting equipment, have been studied extensively (Greacen and Sands 1980; Wästerlund 1992). Studies have tended to take two distinct approaches to the problem of forest harvesting and compaction: (*i*) direct assessment of compaction at a series of points (e.g., Carter et al. 2000) and (*ii*) a stand-level assessment of visible disturbance (as in Lanford and Stokes 1995). Direct measurement of soil compaction provides insight into the relationship between management- or equipment-related factors and soil characteristics. Results are often a model relating traffic density (number of machine passes per unit area) to changes in soil properties. Stand-level studies, on the other hand, evaluate relative measures of harvested area impacted in one of several qualitative categories. The categories are normally assigned visually to speed the measurement process. Neither method provides a complete, meaningful assessment of the degree of impact resulting from harvesting equipment; the direct measurements give results for a specific level of traffic but no idea of how much area was impacted to that degree, and the stand-level measurements are expressed in terms not necessarily related to true changes in soil properties. A method is needed to bridge the gap in these two approaches, one that would ideally "map" changes in soil physical properties across an entire site with high resolution and precision.

McMahon (1997) proposed such a measurement system. Global positioning system (GPS) receivers were used to track machinery, and the results were converted to a raster map with cell values being the number of times a machine crossed that location. Given a model of change in soil properties with number of machine passes, the maps provided a complete record of total impacts to a site and could be applied, for example, in measuring long-term site impacts or

Received 14 February 2001. Accepted 11 October 2001. Published on the NRC Research Press Web site at http://cjfr.nrc.ca on 6 February 2002.

**T.P. McDonald**[1] **and E.A. Carter.** USDA Forest Service, Southern Research Station, G.W. Andrews Laboratory, 520 DeVall Drive, Auburn, AL 36849-5418, U.S.A.
**S.E. Taylor.** Biosystems Engineering Department, Auburn University, Auburn, AL 36849, U.S.A.

[1]Corresponding author (e-mail: tpmcdonald@fs.fed.us).

 DOI: 10.1139/X01-189 

**Fig. 1.** Example of a path segment with its corresponding buffer defining the area of impact. The original path consists of the points labeled *A*, *B*, and *C*. Buffer width is denoted by *w*, and a subscript of *N* indicates a line segment normal. Figure 1*a* is appropriate when the $\angle ABC$ is greater than a specified threshold. The shaded area indicates the portion of the map that would be incremented by one machine pass. Figure 1*b* is for the case when $\angle ABC$ is less than a specified threshold. For that situation the machine is assumed to have reversed direction, and the lightly shaded region received one machine pass, and the heavily shaded area received two.

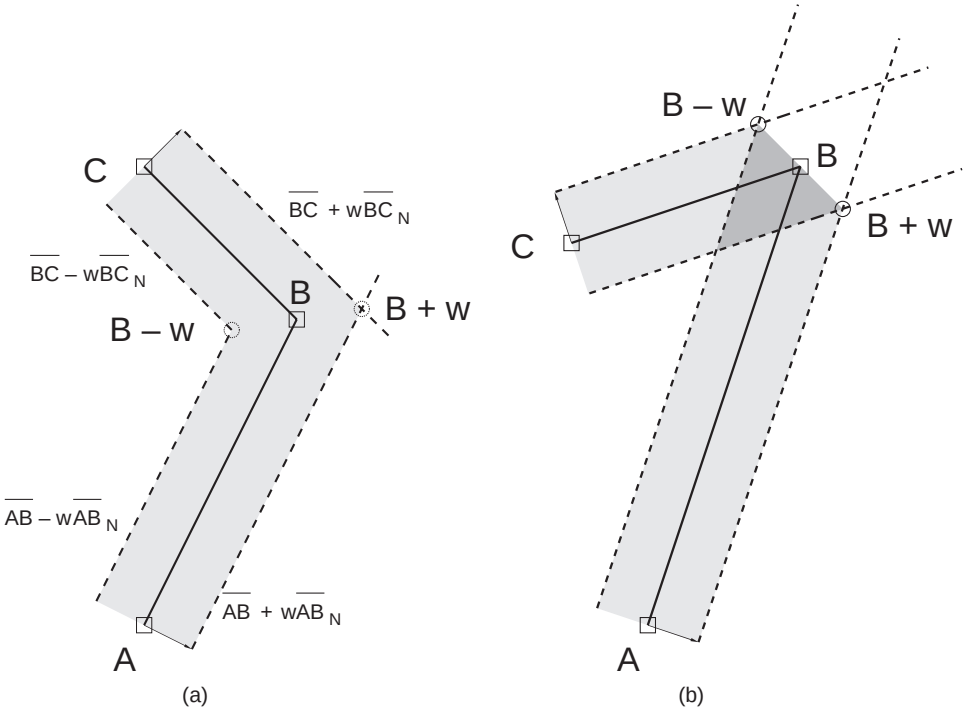


for making decisions on site-preparation tillage requirements.

Given some simplifying assumptions, it is a straightforward process to transform sampled machine positions into a two-dimensional raster map of traffic density. There are, however, many potential sources of error in the transformation that lead to questions of overall accuracy of the maps produced. Quantifying these errors, along with their interactions, is a necessary precursor to using the traffic maps as inputs in management decisions. This paper briefly reviews an implementation of a traffic-mapping system similar to that proposed by McMahon (1997). Errors arising from application of the mapping system in transforming sampled machine positions into a raster map of traffic density are investigated. Finally, results from a study where traffic patterns were monitored on two clear-cut harvests are presented along with a comparison of total impacts measured using the GPS system versus a visual grid sampling approach.

## Materials and methods

### Path rasterization model

For these experiments, a sequence of *x*–*y* pairs representing sampled locations of the centerline of a machine were collected using a GPS at a fixed time interval. These point observations were transformed into a raster map with cell values being how many times the machine passed a given location. The transformation was based on linear interpolation of machine motion between observed locations and on a simple model of the path the machine covered while changing direction. Consider three consecutive machine locations, *A*, *B*, and *C* in Fig. 1*a*. The shaded region was assumed to be that impacted by the machine (or any object with width 2*w*) as it traveled and was bounded by the line segments *AB* and *BC* shifted a distance ±*w* along their respective unit normals. Offset path nodes at point *B* were defined as the intersection of the offset line segments. For angles $\alpha = \angle ABC$, this assumption leads to offset nodes a distance $w/\sin(\alpha)$ from the point *B*, which becomes large for acute angles. It was further assumed, then, that an angle formed between three consecutive positions smaller than some threshold value represented a reversal in direction, rather than a turn. In this case, the impacted area was assumed to be as in Fig. 1*b*, with the lightly shaded area receiving one pass and the heavily shaded area receiving two. The threshold angle used throughout this study was 90°. This algorithm ignored the dynamics of a turning vehicle, including offsets in front and rear axle tracking caused by noncentered articulation points, opting for simplicity instead. A more realistic approach might have been to anchor a point on the side inward of the turn direction, then sweep an arc of constant radius to form the path boundary on the other side. The linear approximation, however, afforded much greater simplicity in implementation, while sacrificing only a small amount of accuracy.

The transformation system was implemented as a set of tools that could perform three fundamental operations on a sampled path: offset a path by a scalar, buffer a path by a scalar amount, and scan rasterization. Offsetting a path involved shifting it along its unit normal a specified distance

**Fig. 2.** A portion of a traffic map for a skidder operating in a tree-length harvesting system. Data were sampled at 0.5 Hz using a Trimble ProXR GPS. Spatial resolution was 0.17 m in both cardinal directions. Inset area shows the data collected over the entire sampling period.


using the algorithm presented in Fig. 1. Buffering a path was the term used to describe the procedure of expanding a linear feature into a polygon. Conceptually, the process could be described as calculating the location of the edges of a road from its centerline, assuming you know its width. The buffering algorithm used in this study applied the offset method described above to a machine path (the centerline), shifting it by a scalar amount to either side to define the edges of a bounding polygon. Rasterization was the process of converting the buffered path from real world coordinates into an image format where pixel values represented number of passes. In the current implementation of the path mapping system, a machine path was processed sequentially from start to finish in short (three position) segments. Each segment of the path was buffered, then mapped into the output traffic density raster. The program user specified an origin for the traffic raster in universal transverse Mercator (UTM) coordinates (top left), a range in the easting and northing directions, a raster size (number of rows and columns in the output image), and a machine or tire width. The range and raster size parameters defined the cell size of the output image. The tire width parameter controlled the width of the calculated path buffer. The mapping program read a path from standard input and generated a raster traffic density map in Portable Graymap (PGM) format.[2]

Figure 2 shows a portion of a buffered path calculated from several hours of data collected from a skidder using a Trimble Pro XR model GPS sampling at 0.5 Hz (1 sample/2 s; GPS settings: C/A code, manual 3D mode, SNR mask 6.0, PDOP mask 8.0; differentially corrected using data from a base station located about 10 km away). Cell size in the image was 0.17 × 0.17 m, and total spatial extent was 1200 m in the east–west direction, 600 m in the north–south, resulting in a 7000 × 3500 pixel raster image. The figure shows a section of the entire map about 220 × 190 m, and traffic intensity was not distinguished. All areas trafficked were shown as open areas to increase the clarity of the picture.

**Error evaluation**

Two primary applications were envisioned for the traffic maps: site-level estimates of total area impacted in various intensity classes and as guides in evaluating traffic impacts at a specified point. For the first case, a definition was needed for the accuracy of the distribution of machine passes over the entire site, whereas for the second a confidence interval was required on the estimated number of passes for a given location. In either case, physically measuring the accuracy parameters was not feasible.

Several methods to physically measure the number of machine passes independently of GPS tracking were explored, but none were found to be simple enough to implement in the field, with the possible exception of using an observer to count passes over a prelocated spot. Although this approach was attempted, the results were less than satisfactory for areas that were not heavily trafficked (basically, off skid trails). It was difficult to define points in locations that would receive few machine passes, then have an observer watching that location when the traffic actually happened. Because of this, it was decided that a simulation approach to defining error effects would be used in this study. The objective in performing the simulations was not to completely define error terms from any possible source but, rather, to

[2] See, for example, http://netpbm.sourceforge.net/ for a description of the PGM format and to obtain a suite of tools for converting among numerous image formats.

**Fig. 3.** A sine curve sampled at 3 (bottom) and 25 (top) samples per period of oscillation, then buffered using the path-mapping algorithm presented in the text.

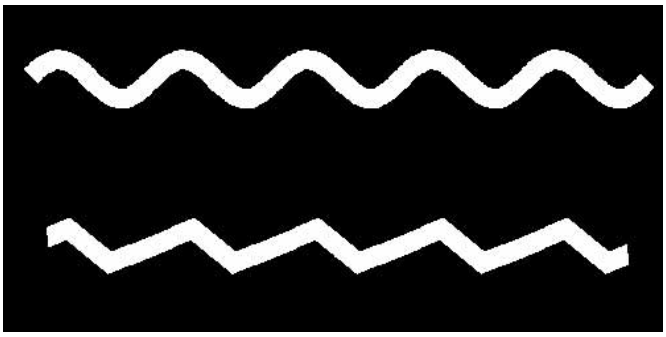

estimate the magnitude of expected errors in a general sense to assist in making decisions about how to improve the overall mapping process.

Errors associated with generating traffic maps were expected to arise from at least three separate sources: (*i*) loss of information resulting from sampling of the machine path, (*ii*) mapping the path into a raster, and (*iii*) errors associated with the GPS, including, among others, those arising from signal loss, changes in satellite constellation, and multipath. The contribution of each of these error sources to the total accuracy was examined individually.

**Movement model and sampling rate**

The location interpolation algorithm described above will approach the true path of the machine as sampling interval goes to zero. Sampling rates above 1 Hz, however, are not generally available with present GPS technology. The following simulation experiment was used to evaluate how a limited sampling rate might affect traffic map accuracy. A series of 11 machine paths were generated from a sine curve. The sine function was sampled at rates ranging from 3 to 25 samples per period of oscillation, for a total length of five periods. Figure 3 shows two examples of a buffered sine wave sampled at 3 and 25 points per period. The total buffered area of this curve, *A*, was given by the following equation:

$$[1] \qquad A = w\int_0^L \sqrt{1 + a^2 \sin^2(x)}\,\mathrm{d}x$$

where *w* was the buffer width, *L* the range in the *x* direction, and *a* the amplitude of the sine wave. For these tests, the buffer width and amplitude of the sine wave were set to one. Raster maps of the buffered sine curve were made using the path mapping system and raster areas compared to that calculated from eq. 1. Pixel size was approximately 7% of the path width (ratio of buffer width/pixel size = 16).

**Raster resolution**

Another important factor influencing the accuracy of the traffic maps was the resolution of the output raster. Accuracy of the raster maps would be expected to decrease as pixel sizes approached the path buffer width. An experiment was conducted to examine the effects of output raster resolution in which a series of six test images were generated, each from 25 pairs of points randomly located along the perimeter of a 10 × 10 unit square. Each point pair defined the endpoints of a straight-line path. Each linear path was buffered using a rectangular polygon 0.2 units in width. Figure 4 shows an example of one of the test images. Each test image was generated using a different raster resolution. Resolution was expressed as a ratio of buffer width to pixel size and ranged from 0.3 to 10. For this type of simple image, it was possible to directly calculate areas of all polygons resulting from the intersecting rectangles and compare those values to areas measured from the rasterized maps.

**Fig. 4.** Example of a test image used in evaluating the effect of sampling resolution on path-mapping accuracy.

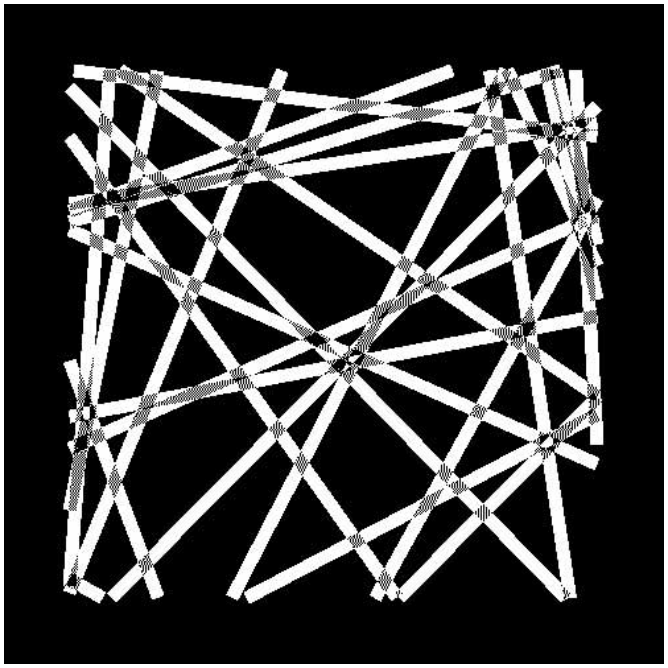

**GPS errors**

Pointwise accuracy of GPS positions is influenced by a great many factors and is normally expressed as an expected residual from a known location (Brock and Karakurt 1999; Karsky et al. 1999; Veal et al. 2000). The magnitude of the residual, depending on the type of GPS receiver used and the conditions in which it was operated, typically ranges from one to several skidder tire widths, implying that GPS errors significantly influence the overall accuracy of traffic density maps.

An empirical assessment of the effect of GPS errors on point-level estimates of traffic density was made using the data set a portion of which is shown in Fig. 2. The traffic map as shown in the figure was assumed to be completely accurate. Data used to derive the figure were altered, then traffic maps reproduced and compared with the original. The original data were altered by adding a random offset to each GPS position. Offsets were assumed to be independent in the east–west and north–south directions, errors in both directions normally distributed with a mean of zero and known variance. Traffic maps derived from the offset data were compared on a point-by-point basis to the unaltered version, and the probabilities of an individual pixel having the same

value in both images were calculated. One map was generated for additional errors of 0.5, 1.0, and 1.5 $m^2$ mean variation in sample position.

Accuracy of the simulated traffic images was evaluated in two ways. Distributions of total image area by number of passes were generated and compared with values either calculated directly or with those for a reference image. Total areas, however, did not describe misclassification errors or how often a specific pixel was assigned a value $n$ when it should have been $k$. This type of error for an image $A'$ was evaluated relative to a reference image $A$ using the measure $G_{d,k}$:

$$[2] \qquad G_{d,k} = \frac{v[(A' - A)_d \bigcap A_k]}{v(A_k)}$$

where $d = n - k = 0, 1, 2, \ldots$, $A_k$ was the subset of the image $A$ having value $k$, and $v(A)$ was the area measure on $A$. Values of $G$ represented a misclassification rate for a given number of passes. For example, the value of $G_{0,k}$ was the proportion of pixels in $A$ with value $k$ that also had value $k$ in image $A'$. Similarly, $G_{1,k}$ was the proportion of $A$ with value $k$ that had value $k + 1$ in $A'$. The measure is similar conceptually to an error matrix (Prisley and Smith 1987), with the $G_{0,k}$ values representing the error matrix diagonal, and off-diagonal values being an error relative to the original values. Since there were areas of hundreds of passes, the use of an error matrix would have been unwieldy, and the use of $G_{d,k}$ simply provided a more succinct way of expressing the relevant results.

### Field tests of GPS mapping

Most traffic from harvesting machinery was monitored on a 16.4-ha, clearcut, 20-year-old loblolly pine (*Pinus taeda* L.) plantation in Lee County, Alabama, in February–March 1998. The logger used a single feller–buncher and two skidders pulling to two loaders. Conditions were generally wet during the harvest. Traffic data were collected using 2 Trimble ProXR receivers (12-channel L1C/A receiver, 1 m typical accuracy) on the skidders, and a Trimble GeoExplorer II (6-channel L1 C/A receiver, 2–5 m typical accuracy) on the feller–buncher. All systems sampled position once every 2 s. Reliability of the GPS systems was generally good, but short-term losses were common because of recurring battery and antenna mounting problems, especially for GPS receivers mounted on the feller–buncher.

Following harvest, site disturbance was estimated using a visual inspection method. The surface characteristics listed in Table 1 were evaluated on a chain-by-chain grid by a trained observer. These characteristics were used to classify the harvested area into the categories shown in Table 2.

GPS traffic data were transformed, using the algorithm presented above, into a georeferenced raster image with 0.5 × 0.5 m cell size. The image was further classified into disturbance classes based on number of passes (Table 2). The class definitions were chosen to correspond to the results found in the visual survey for the "disturbed" and "slightly disturbed" categories, allowing a comparison of the methods at the extremes of traffic damage, i.e., undisturbed or in skid trails and decks. This was purely a practical choice not based on available literature or theory.

**Table 1.** Visual features recorded in grid-sampled site disturbance classification.

| Type of disturbance | Disturbance characteristic |
|---|---|
| Soil disturbance | (A) Litter in place |
| | (B) Mineral soil visible |
| | (C) Mineral soil only |
| | (D) Mineral soil and litter mixed |
| Traffic | Deck |
| | Primary skid trail |
| | Secondary skid trail |
| | Nontrail trafficked |
| | Untrafficked |
| Ruts | <5 cm |
| | >5 cm |

**Table 2.** Relationship between observed disturbance characteristics, definition of disturbance classes, and the relationship used to compare visual disturbance with number of passes calculated from the GPS data.

| Disturbance class | Characteristic | No. of passes |
|---|---|---|
| Undisturbed | Untrafficked | 0 |
| Decks and trails | Skid trail primary, secondary deck | 21+ |
| Disturbed | Soil disturbance B–D, any rut level | 4–20 |
| | Soil disturbance A, ruts >5 cm | |
| Slightly disturbed | Soil disturbance A, ruts <5 cm | 1–3 |

## Results and discussion

### Movement model and sampling rate

A sine curve was sampled at varying frequencies, then a buffered curve created using the path mapping algorithm. Trafficked area measured from the resulting image was compared with the theoretical area calculated from eq. 1. Table 3 summarizes the difference in calculated total area covered and that derived from applying the path rasterization technique for different sampling rates. In this example, there was not any appreciable loss in accuracy for sampling rates higher than about six times per period of the sine wave. This made sense in that a minimal level of information about the path would be required to simulate it linearly: a start, a maximum, and an ending point for each halfwave, or five points per period of oscillation (ending and beginning point of each successive period were the same).

Total area covered, however, was not fully representative of the degree of inaccuracy in the resulting images, providing no information on the amount of area misclassified, that is should have been value $k$ but was instead $n$ ($n = d + k$). Assuming the image generated from the highest sampling rate (25 samples per period in this case) was the "correct" version ($A$ from eq. 2), Table 4 shows the correspondence of individual pixels ($G_{d,k}$) as a function of sampling frequency. Because pixels in the image could have a value of only zero or one, there were just two types of errors possible. A pixel from an image sampled at a lower rate could have a value of zero when the same pixel in the reference image (sampled at

25 samples per period) had a value of one ($d = 0 - 1$, $G_{-1,1}$), and vice versa (value of one with corresponding pixel in the reference image having value of zero, or $G_{1,0}$). The results from the table confirm the earlier conclusion based on the total image areas that there was not a large improvement in overall accuracy for the paths sampled at rates higher than six times per period of oscillation. The difference from the previous results, however, was the degree of inaccuracy found when expressed as a percentage of area misclassified. Relative to the 25 samples per period image, almost 30% of the total "trafficked" area was misclassified for the image generated from three samples per period. From these results it was concluded that total trafficked area was not sensitive to errors resulting from path sampling rate deficiencies but that error rates for individual pixels could be high with an insufficient sampling rate. The use of GPS data in estimating total area trafficked from skidder movements, therefore, would not be adversely affected by using sampling rates lower than might be optimal to capture true machine motion. Skidder movements are not that abrupt relative to the highest sampling rate possible with most GPS units (1 sample/s): they tend to travel in straight lines without sharp turns. For tracking impacts from feller–bunchers, however, a higher sampling rate may be necessary since their motion can be much more variable over short distances and time periods.

Also evident from the results was that error rates did not go to zero as the sampling rate approached that of the "true" image. The 0.5% difference in misclassified pixels between the 20 and 25 samples per period images was probably the result of edge effects along the buffered path. Individual pixels along the edges of the two paths differed because of an aliasing effect, similar to rounding errors. Although a simple antialiasing scheme was built into the path rasterization algorithm, it did not completely prevent these types of differences, the degree of which would depend on the resolution of the images and the traffic density at a given point.

**Table 3.** Comparison of total trafficked area for the same sinusoidal path using different sampling rates.

| Samples per period | Percent difference in calculated and measured area |
|---|---|
| 3 | 5.06 |
| 4 | 2.92 |
| 5 | 2.66 |
| 6 | 2.83 |
| 7 | 1.04 |
| 8 | 1.60 |
| 9 | 1.36 |
| 10 | 0.74 |
| 15 | 0.50 |
| 20 | 0.53 |
| 25 | 0.51 |

**Note:** Difference is area measured from the raster-mapped path with the area calculated from eq. 1.

**Table 4.** Values of the parameter $G_{d,k}$ for a sinusoidal path sampled at various frequencies.

| Sampling rate (samples per period) | $G_{-1,1}$ | $G_{1,0}$ | Correctly classified |
|---|---|---|---|
| 3 | 0.123 | 0.163 | 0.714 |
| 4 | 0.088 | 0.110 | 0.802 |
| 5 | 0.051 | 0.071 | 0.878 |
| 6 | 0.046 | 0.068 | 0.886 |
| 7 | 0.027 | 0.032 | 0.941 |
| 8 | 0.024 | 0.035 | 0.941 |
| 9 | 0.022 | 0.030 | 0.948 |
| 10 | 0.020 | 0.022 | 0.958 |
| 15 | 0.019 | 0.019 | 0.962 |
| 20 | 0.026 | 0.016 | 0.958 |

**Note:** The indices $d$ and $k$ refer to those pixels in an image $A$ having value $k$, but had value $n$ in a transformed image $A'$, with $d = n - k$, $d = 0, 1, 2, \ldots$, the difference in value between the same two pixels. For this comparison, the reference image $A$ was derived from sampling the sine wave at 25 samples per period of oscillation.

## Raster resolution

Comparison of image-derived versus directly calculated intersection areas are presented in Table 5 for several image resolutions. The results showed that resolution did not greatly influence the overall accuracy of predicted area, although there were differences by number of passes. Even for pixel sizes over three times larger than the buffer width (resolution = 0.3), the predicted areas were within 15% of the actual values by number of passes (difference in "direct" and "image" areas, up to two passes), and within 10% for total area. At lower resolutions, however, areas of higher order intersections (above 2 for the resolution = 0.3 case) were not identified.

It appeared from the results in Table 5 that pixel sizes should be on the order of one-fifth the path width to identify all intersections accurately. This should vary, however, given the relative size of intersecting path buffers, which should, in turn, be influenced by the number of intersecting paths in a given area. It is likely that for areas of dense traffic, pixel sizes of (path width)/(highest order of intersection) would be required to get accurate values for intersection area. For typical tree-length logging systems, areas of dense traffic are small relative to the entire harvest unit size. Machine passes near decks could easily be in the hundreds, requiring a very high resolution for absolute accuracy. Such a high resolution would require a very large output raster that would be impractical to store, manipulate, and view. A compromise resolution would combine a feasible output image size and provide acceptable spatial accuracy. Typical wheel widths on forest harvesting equipment in the southern United States are about 1 m, and for regions somewhat removed from the deck a typical maximum number of passes at a given spot might be on the order of five. This would suggest a pixel size on the order of 0.2 m. For a harvest unit that fit within a 1-km square region, using the 0.2-m resolution would result in a 5000 × 5000 pixel output raster size. This is a reasonable size to store and analyze, although it is not easy to display or print a picture that large. If greater accuracy is required, perhaps a vector approach could be used to reduce the amount of data, although this could make the calculations much more intensive.

## GPS errors

Comparisons were made between the data, a portion of which is shown in Fig. 2 (image $A$ in eq. 2), and an image ($A'$ in

**Table 5.** Comparison of actual and image-derived area for a series of rectangles (see Fig. 4).

| Intersection level | Resolution = 10 | | Resolution = 5 | | Resolution = 2 | | Resolution = 1 | | Resolution = 0.5 | | Resolution = 0.3 | |
|---|---|---|---|---|---|---|---|---|---|---|---|---|
| (no. of passes) | Direct | Image | Direct | Image | Direct | Image | Direct | Image | Direct | Image | Direct | Image |
| 1 | 20.732 | 20.712 | 18.240 | 18.142 | 20.976 | 20.780 | 18.958 | 19.440 | 19.157 | 17.440 | 19.477 | 17.777 |
| 2 | 5.549 | 5.562 | 4.545 | 4.622 | 5.612 | 5.760 | 4.575 | 4.120 | 4.490 | 4.800 | 3.915 | 4.444 |
| 3 | 0.703 | 0.707 | 1.189 | 1.195 | 0.883 | 0.870 | 1.050 | 0.840 | 1.086 | 0.800 | 0.829 | 0.000 |
| 4 | 0.037 | 0.035 | 0.269 | 0.274 | 0.036 | 0.040 | 0.172 | 0.240 | 0.169 | 0.320 | 0.292 | 0.000 |
| 5 | 0.000 | 0.000 | 0.032 | 0.026 | 0.001 | 0.000 | 0.002 | 0.000 | 0.012 | 0.000 | 0.040 | 0.000 |
| Difference (total area, %) | 0.02 | | 0.07 | | 0.20 | | 0.50 | | 6.2 | | 9.5 | |

**Note:** Images varied in resolution, which is expressed as the ratio path buffer width/pixel size.

eq. 2) derived from the same GPS data as Fig. 2, but with each value offset by a random amount. Offsets were normally distributed in the east–west and north–south directions with mean 0 and variance $v$ = 0.5, 1.0, and 1.5 m$^2$. Expressed in polar coordinates, the offset angle was uniformly distributed, and the radial distance from the original value had a mean of about $1.25v^{0.5}$(0.88, 1.25, 1.53 m).

Total trafficked area increased with higher point offset variance, 13.5% for a variance of 0.5 m$^2$, 23.8% for 1.0 m$^2$, and 29.2% for 1.5 m$^2$. Most of the difference was in regions of one to seven passes (Fig. 5), with increasing variance resulting in a higher total area trafficked up to about 10 passes. Area of regions trafficked more than 10 passes was lower for all three perturbed images. The distribution of number of passes was similar in all cases (Fig. 6), with increasing variation in individual GPS positions showing a somewhat higher percentage of areas trafficked from 2 to 5 times, and a lower percentage of regions crossed 1 and more than 10 times. Adding random perturbations to each position represented a kind of dilution effect. Larger errors tended to spread the same "amount" of traffic over slightly greater areas, tending to increase overlap between machine trips in areas of few passes and decrease it in areas of relatively high numbers of passes.

These results implied that errors in GPS positions resulted in somewhat higher estimates of total area trafficked but were relatively constant in the proportion of the trafficked area in the same traffic class (having the same number of passes). If the objective in mapping traffic was to assess the relative proportions of a harvest tract that were impacted, the presence of random fluctuations in GPS positions should be minimized, but results should be reasonable even in the presence of moderate variation in individual positions. Again, however, these results did not indicate the probability that any single point in the unit was crossed a given number of times.

Table 6 shows the proportion of the data a portion of which is shown in Fig. 2 with pixel values 1–5 that had the same value in the perturbed image, or differed by ±1. The proportion of all points that ended up with the same value following the perturbation of the GPS data was less than 40% in all cases, and was lower for increasing numbers of passes. The number of pixels identified as being within ±1 pass of the original value was generally 1.5 to 2 times higher and was also less for higher numbers of passes. There was a 76–85% chance that a location identified as originally having received one pass would have between zero and two passes after the additional error was included. The probabilities dropped significantly, however, when the location was originally hit five times: there was only a 44–50% chance that the same point in the perturbed images would have from four to six passes.

## Field testing

Figure 7 shows the final traffic density map for the clearcut site. There were two extended periods of time where data from the feller–buncher were lost, and these areas were excluded from the analysis, reducing the final area to 11.1 ha. The traffic measures were compared with grid samples collected over the entire 16.4-ha site. Table 7 is a comparison of percent area in visually determined disturbance classes

**Fig. 5.** Total trafficked area by number of passes and amount of random variation added to individual data points.

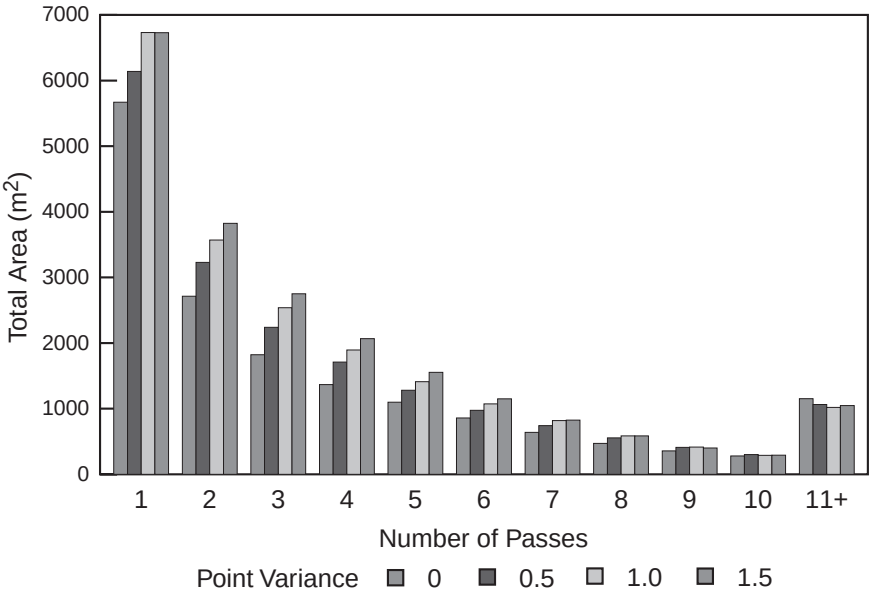


**Fig. 6.** Distribution of number of passes of the same skidder path with four levels of random variation added to individual locations.

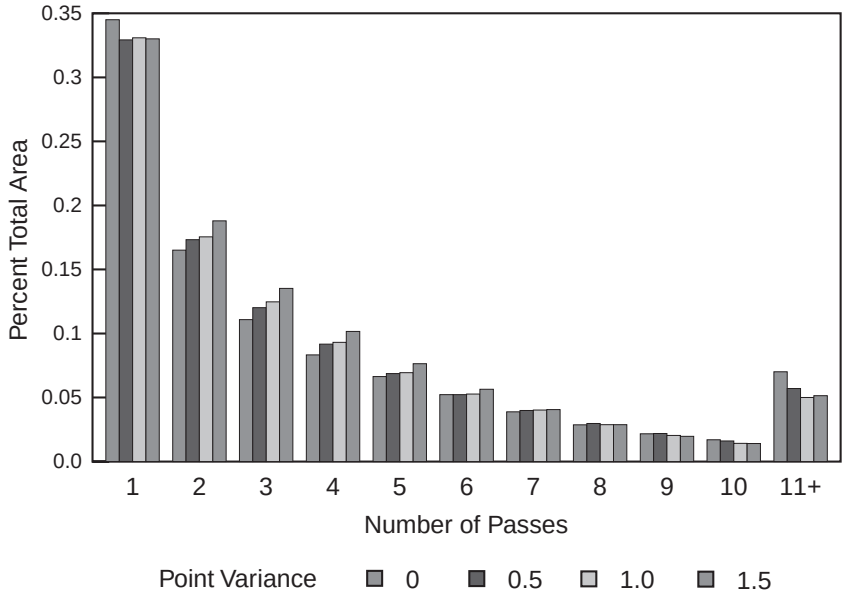


**Table 6.** Table of $G_{d,k}$ values, where $k$ is the number of passes in the original (correct) image and $d$ is the difference between the value of the same pixel in a perturbed image.

| | Variance = 0.5 m$^2$ | | Variance = 1.0 m$^2$ | | Variance = 1.5 m$^2$ | |
|---|---|---|---|---|---|---|
| $k$ | $d$ = 0 | $d$ = ±1 | $d$ = 0 | $d$ = ±1 | $d$ = 0 | $d$ = ±1 |
| 1 | 0.35 | 0.50 | 0.33 | 0.47 | 0.27 | 0.49 |
| 2 | 0.26 | 0.42 | 0.23 | 0.40 | 0.21 | 0.38 |
| 3 | 0.22 | 0.39 | 0.21 | 0.36 | 0.19 | 0.35 |
| 4 | 0.20 | 0.35 | 0.18 | 0.33 | 0.18 | 0.32 |
| 5 | 0.17 | 0.33 | 0.15 | 0.31 | 0.15 | 0.29 |

**Note:** The table values are the proportion of pixels in an image where the sampled machine positions have been varied by a random amount (variance = 0.5, 1.0, and 1.5 m$^2$) that were the same ($d$ = 0) or differed by 1 ($d$ = ±1) from the original image.

and in the same classes defined from numbers of passes using the GPS maps. The visual disturbance method overestimated the area in decks and trails and underestimated the undisturbed area relative to the GPS mapping procedures. This result was consistent with previous published reports (McMahon 1995) showing that accurate grid-sampled estimates of area by disturbance class require a much higher sampling density than the chain-by-chain grid used in this study. Part of the difference was due to the fact that the path mapping system measured area trafficked only. Felling and dragging trees can cause visible disturbance independent of machine traffic. The main difference in the two methods, however, was likely due to how untrafficked and heavily trafficked areas were distributed over the site. Other analysis (McDonald et al. 1998) found that over half of all untrafficked areas were in small, dispersed patches (less than

**Fig. 7.** Traffic density by disturbance class (based on number of passes) on harvested site. Data are included for all traffic (feller–buncher and skidder). Total area was 11.1 ha.

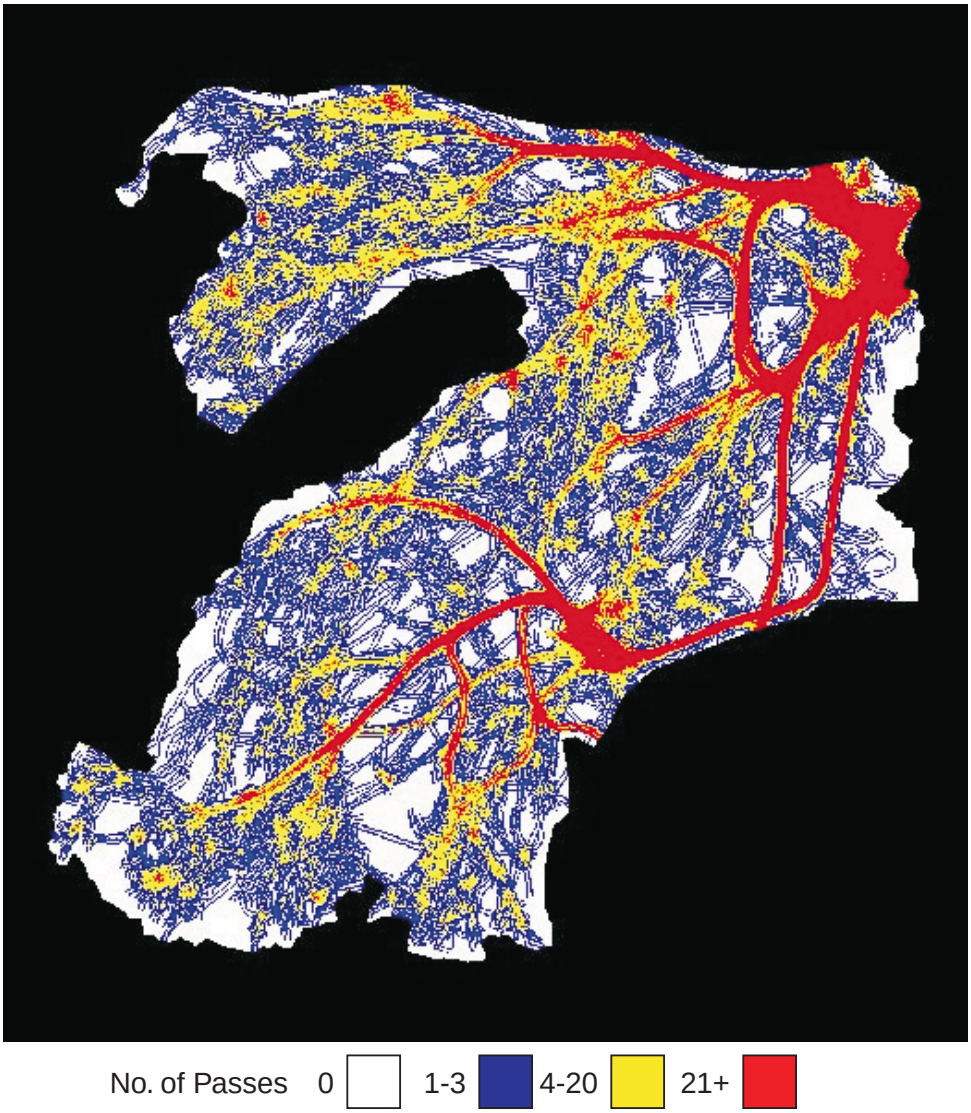


**Table 7.** A summary of percent area of the stand by visual disturbance class, with associated estimate based on number of passes.

| | Percent area | |
|---|---|---|
| Disturbance class | Visual | GPS |
| Undisturbed | 9.5 | 27.9 |
| Slightly disturbed | 37.5 | 37.9 |
| Disturbed | 27.0 | 29.2 |
| Decks and trails | 18.5 | 5.0 |

**Note:** Total visually assessed disturbed area does not include nonsoil locations (slash piles, stumps, rocks, which accounted for 7.5% of the total area).

3.5 m in diameter), areas that were no more likely to be randomly included in a wide sampling grid than any other spot. Disturbed areas, on the other hand, were concentrated in specific areas and highly spatially correlated. If, for example, a grid line happened to fall along a skid trail, many samples on that line would be classified as trail.

It should be noted that the conditions under which the data for this study were collected represent a best-case scenario. Accuracy of raw GPS data can be severely degraded when collected under a canopy, as in a partial harvest. Equipment characteristics can also impact tracking accuracy, especially for machines equipped with booms that can block signals or cause multipathing problems. The generation of traffic maps using GPS requires enormous amounts of raw position data that can be a burden to collect and also to edit when there are numerous erroneous readings present.

Despite some drawbacks, GPS mapping of disturbance was a practical means of tracking impacts from harvest over long periods of time. With improvements in GPS and communications technology, the data collection systems could be more robust and easily accessible, making the generation of traffic maps nearly an autonomous process. The data could be useful in predicting areas to receive spot cultivation or

fertilization to counteract the effects of machine traffic. The maps also provide a long-term record of impacts to a site that could be important in addressing sustainability issues. The machine traffic data might also be useful in other contexts, in optimizing harvesting efficiency, for example.

## Conclusions

These results indicated that traffic maps produced from GPS data were not well suited for analysis involving point-level estimates of traffic density. In particular, using the maps to direct soil sampling for specific numbers of passes would be inappropriate. Better results would be achieved if numbers of passes were lumped into categories. In that case, the likelihood that any particular point was in a specific traffic density class would be high enough to justify some level of confidence in the results.

Taken cumulatively, the outlined procedures resulted in maps that were acceptable for answering site-level disturbance questions. For example, assessing the total area trafficked would likely be reasonably accurate if sufficient control was exercised in collecting the raw GPS positions, such as proper position dilution of precision masking, elevation masking, etc. Identifying number of machine passes at a given point, however, would be suspect. The method should be appropriate for use in comparing traffic intensity across sites. If maps for multiple sites were generated in an identical fashion, traffic patterns in given classes should have similar levels of error and be comparable. This would make it possible to compare impacts of different machinery systems, for example, or the effect of topography on impacts from traffic. Further research is needed to more precisely define confidence intervals on point-level estimates of numbers of passes, which should vary significantly with the instrumentation and machinery systems used and, therefore, be valid only in very restrictive circumstances.

Application of the method in long-term monitoring of harvest impacts was demonstrated and shown to provide results that correlated well with visual assessments of site disturbance. The mapping approach provided the additional benefit of showing where the impacts occurred, and as raster layers in a GIS the traffic data could be used in further analyses, such as correlating growth impacts with harvesting traffic on regenerated stands, or measurements of the size distribution of trafficked or untrafficked areas.

## References

Brock, R.H., and Karakut, E. 1999. GPS precision and efficiency under variable forest types and crown density. American Society of Agricultural Engineers, St. Joseph, Mich. Am. Soc. Agric. Eng. Pap. 95035.

Carter, E., McDonald, T., and Torbert, J. 2000. Assessment of soil strength variability in a harvested loblolly pine plantation in the Piedmont region of Alabama, United States. N.Z. J. For. Sci. **30**(1/2): 237–249.

Greacen, E.L., and Sands, R. 1980. Compaction of forest soils. A review. Aust. J. Soil Res. **18**: 163–189.

Karsky, D., Patterson, D., and Jasumback, T. 1999. Evaluating the Trimble ProXRS GPS receiver using satellite realtime DGPS correction. Engineering Tech Tips. May 1999. USDA Forest Service, Missoula, Mont. Rep. 9971-2318-MTDC.

Lanford, B.L., and Stokes, B.J. 1995. Comparison of two thinning systems. Part 1. Stand and site impacts. For. Prod. J. **45**(5): 74–79.

McDonald, T., Carter, E., Taylor, S., and Torbert, J. 1998. Relationship between site disturbance and forest harvesting equipment traffic. *In* Proceedings of the 2nd Southern Forestry GIS Conference, 28–29 Oct. 1998, Athens, Ga. Warnell School of Forest Resources, Athens, Ga. pp. 85–92.

McMahon, S. 1995. Accuracy of two ground survey methods for assessing site disturbance. J. For. Eng. **6**(2): 27–32.

McMahon, S.D. 1997. Unearthing soil compaction: the hidden effects of logging. GPS World, **8**(March): 40–45.

Prisley, S.P., and Smith, J.L. 1987. Using classification error matrices to improve the accuracy of weighted landcover models. Photogram. Eng. Remote Sens. **53**: 1259–1263.

Veal, M.W., Taylor, S.E., McDonald, T.P., Tackett, D.K., and Dunn, M.R. 2000. Accuracy of tracking forest machines with GPS. American Society of Agricultural Engineers, St. Joseph, Mich. Am. Soc. Agric. Eng. Pap. 005010.

Wästerlund, I. 1992. Extent and causes of site damage due to forestry traffic. Scand. J. For. Res. **7**: 135–142.